Optical Properties of Tissue in Near-infrared Region for NIRS-based Medical Imaging

Manob Jyoti Saikia[a]

[a]Electrical Engineering, University of North Florida, Jacksonville, FL 32224, USA

ABSTRACT

The optical properties and physiology of biological tissue, as well as how near-infrared (NIR) light interacts with the tissue, both play a significant role in interpreting the tissue probing optical measurements, and in solving the inverse problem of near-infrared spectroscopy (NIRS)-based medical imaging modalities such as diffuse optical tomography and functional near-infrared spectroscopy. This paper discusses the optical properties of tissue, specifically in the NIR wavelength range, which influence NIRS measurements in NIRS-based medical imaging. There is an easy-to-understand explanation given in this paper of the NIR light-tissue interaction phenomenon. The mathematical explanation, the processes involved in the interaction, and the rationale for a few approximations are described. Various types of chromophores present in the tissue, their composition in the tissue, and how these chromophores overall affect the scattering and absorption of NIR light are presented. The absorption spectra of these chromophores are shown. Finally, the paper concludes with the author's perspective on two NIRS-based medical imaging modalities, diffuse optical tomography, and functional near-infrared spectroscopy.

Keywords: near-infrared; spectroscopy; tissue; medical imaging; diffuse optical tomography; fNIRS

1. INTRODUCTION

Understanding the optical properties and physiology of the tissue is essential to interpret near-infrared spectroscopy (NIRS)-based optical measurements for medical imaging such as diffuse optical tomography (DOT) for breast imaging and functional near-infrared spectroscopy (fNIRS) for brain imaging. A traditional way of modeling the propagation of electromagnetic waves in a medium is by using Maxwell's equation. Due to the strong scattering of light in the near-infrared (NIR) region, a detailed description is not necessary since wave properties such as polarization and interference can be ignored once the light traverses a few millimeters of tissue. There is a possibility that light-tissue interactions can alter the structure of the tissue or even destroy it. Phototherapy and laser surgery are examples of medical procedures in which interaction mechanisms like these are used.[1] The origin of optical spectroscopic parameter distributions and the interaction of light with optical parameters in tissue media are characterized by photon transport. Optical parameter distribution-based imaging modalities[2–10] uses NIR light which propagates through the tissue volume and carries with it quantitative information[4,11,12] about physiological changes that occur in living biological tissues.

Optical medical imaging has low-intensity levels, a few mW/mm^2, which prevent any tissue destructive processes from occurring. Fluorescence, phosphorescence, and Raman scattering do not have a significant effect on NIR light propagation due to inelastic scattering. Absorption and scattering are the two optical phenomena that mostly determine how photons behave and travel through tissues.[13] Despite the importance of both mechanisms, scattering dominates in the tissue.[14] It is likely that injected photons scatter at least several times before reaching a boundary in tissue objects, even for a thin sub-millimeter section of a tissue sample. Generally, the way light is transported inside a tissue is characterized by a combination of two optical parameters called the absorption coefficient (μ_a) and scattering coefficient (μ_s) along with a factor referred to as scattering anisotropy (g). A photon's probability of being absorbed in an infinitesimal path length is given by the absorption coefficient, μ_a in mm^{-1}. A scattering coefficient, μ_s in mm^{-1}, indicates the probability of a photon scattering in an infinitesimal path length. The cosine of the scattering phase function is the anisotropic factor (g).

Send correspondence to Manob Jyoti Saikia
E-mail: manob.saikia@unf.edu

Preprints (www.preprints.org) | NOT PEER-REVIEWED | Posted: 12 December 2022 doi:10.20944/preprints202212.0187.v1

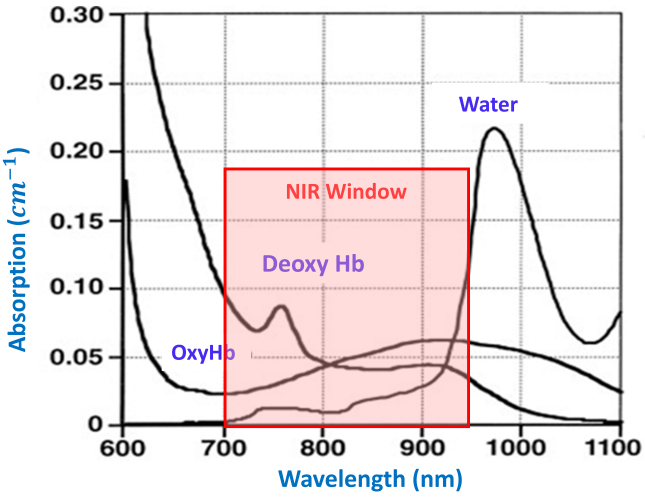

Figure 1. Absorption spectra of major chromophores.

2. OPTICAL PROPERTIES OF TISSUE

2.1 Absorption

Chromophores are special groups of molecules that contribute to light absorption in tissues. Water, hemoglobin, and lipids are the most dominant and well-known chromophores in tissue. The human body consists of approximately 75 % water.[15] As with water, lipids have similar properties in terms of absorption. Depending on the location within the body, lipids make up 1% to 80 % of tissue.[15] Due to the fact that they are typically present at lower relative concentrations, lipids do not generally contribute significantly to the attenuation of total light. Adipose (fat) tissue, such as that in the breast, is primarily composed of lipids, so this rule does not apply. Located over the pectoral muscles of the chest wall, the breast consists of glandular, fat, and fibrous tissue. Fibrous strands known as Cooper's ligaments secure it to the chest wall.[16] The breast glands are surrounded by fatty tissue, which extends throughout the breast. Breasts have a soft consistency due to fatty tissue. It is possible for hemoglobin concentrations to vary significantly at local levels in the tissue. Since deoxygenated (Hb) and oxygenated (HbO_2) hemoglobin have distinctly different NIR absorption spectrums, their absorption properties are dependent on the oxygenation state.[17–20] Functional NIR imaging of tissue relies on these properties. Background absorbers consist of substances with several weak absorbers.

Depending on the type of host molecule, pH level, and temperature, chromophores can have different absorption properties, which can also be affected by environmental factors. The specific extinction coefficient can be used to characterize the absorption properties of a chromophore $\varepsilon^{'}$ $(mm^{-1}mM^{-1})$. The product $C_s\varepsilon^{'}$, where C_s being the concentration of the absorbing compound (mM = mil) is the probability of a photon that is absorbed within a unit length in the medium and is given in mm^{-1}. The Beer-Lambert law gives the intensity of light (I) as a function of path length (x) for a single absorbing compound without scattering, as follows,

$$I(x) = I_0 e^{(-\mu_a x)} \tag{1}$$

where I_o is the intensity of the incident light.

There can be variations in absorber concentrations both spatially and temporally, and extinction coefficients are usually wavelength-dependent. In order to express the absorption coefficient, we use the cross-sectional area per volume of the medium, since several chromophores contribute to the total absorption,

$$\mu_a(x,t,\lambda) = \ln(10) \sum_i C_s^i(x,t)\varepsilon_i^{'}(\lambda) \tag{2}$$

Preprints (www.preprints.org) | NOT PEER-REVIEWED | Posted: 12 December 2022 doi:10.20944/preprints202212.0187.v1

The specific extinction coefficient is defined by using base 10 logarithms. μ_a using the natural logarithm. Water molecules, oxygenated and deoxygenated hemoglobin are the major light-absorbing tissue chromophores and their contributions to overall absorption in the NIR window, in the wavelength range 600 - 890 nm, are significantly different. When we examine the water absorption spectra of the major tissue chromophores (Figure 1), we find that the absorption is quite low in the NIR region of the spectrum. Also, the oxygenated and deoxygenated hemoglobin crossover at a certain point as seen in the (Figure 1).

2.2 Scattering

In the NIR region, elastic scattering is the nature of the interaction between tissue and light. This is because the energy of a photon remains constant but the direction in which it is scattered varies. Light propagation in tissues can be modeled using scattering theories.[6,21–23] Cells and cellular organelles are scattering centers in biological tissues. An imaging window uses a wavelength-equivalent spectral window for cellular organelles. The cytosol and extracellular fluid's index of refraction are comparable. Therefore, tissue scatters light mainly in a forward direction and shows weak wavelength dependence.

The reduced scattering coefficient describes the scattering properties of strongly scattering media ($\mu_s^{'}$), usually expressed in mm^{-1}, it describes the probability that a photon is scattered per unit length. It typically takes a photon a few millimeters or less to lose the memory of its initial direction of propagation in tissues. A single scattering event can be described by an exponential attenuation law similar to Equation 1. In larger volumes of tissue, multiple-scattering effects must be considered, requiring more complex modeling.[21,22] Scattering due to a single particle is expressed by a scattering cross-section σs (mm^2) where the scattering cross-section is a hypothetical surface that explains the likelihood of light being scattered by a scattering particle. The total scattering coefficient μs of a tissue medium made of different scatterers is given by,

$$\mu_s = \sum_i \sigma_s^i \frac{P_i}{V} \tag{3}$$

where P_i is the number of scatterers in a volume V.

Scattering in tissue is usually anisotropic and occurs due to a change in refractive index (n) between the two boundaries. In tissues, such boundaries exist, for instance, between intracellular and extracellular fluids and between the cytoplasm and organelle fluids. Generally, most tissues have refractive indices of around 1.4, which is fairly small on a macroscopic scale.

.[24] Significant differences can be observed at the air-skin interface. It is possible that some tissues have a preferential direction for light propagation due to their macroscopic structure. For example, the structural anisotropy of muscle fibers causes light to propagate along them.[25] The anisotropy factor (g) is usually measured by using the statistical mean of the cosine of the angle between the incident $(\hat{e}_s)$ and scattering direction $(\hat{e_s^{'}})$which is given by,

$$g = 2\pi \int_{-1}^{1} cos\theta f_{\hat{e_s}}(\hat{e_s}, \hat{e_s^{'}}) d\hat{e_s^{'}} \tag{4}$$

Here, $f_{\hat{e}_s}(\hat{e}_s, \widehat{e_s^{'}})$ is the probability function of a photon incident along $\hat{e}_s$, and is scattered along $\widehat{e_s^{'}}$. The typical value of g in soft tissue is 0.9 which implies that scattering is essentially in the forward direction. For $g = 0$, the scattering is fully isotropic. As long as scattering is anisotropic, a reduced scattering coefficient can be used to describe the effective scattering properties of a medium with respect to scattering and is defined as $\mu_s^{'} = (1 - g)\mu_s$.

Table 1 presents the absorption (μ_a in cm^{-1}) and scattering ($\mu_s^{'}$ in cm^{-1}) coefficient of various breast tissue type at wavelength 700 nm.

Preprints (www.preprints.org) | NOT PEER-REVIEWED | Posted: 12 December 2022 doi:10.20944/preprints202212.0187.v1

Table 1. The optical properties of breast tissue at wavelength 700 nm.

Tissue type	$\mu_a(cm^{-1})$	$\mu_s^{'}(cm^{-1})$
Breast, glandular	0.5	14
Breast, adipose	0.7	9
Breast, fibrocystic	0.2	13
Breast, fibrodema	0.5	7
Breast, ductal carcinoma	0.5	12

3. OPTICAL PROPERTIES OF VARIOUS CHROMOPHORES

There are three main constituents of biological tissue that contribute to the absorption of radiation in the near-infrared region: water, lipids, and hemoglobin. In contrast to the former two, oxygenated and deoxygenated hemoglobin concentrations vary with the function and metabolism of the tissue over short time scales. Thus, clinically useful physiological information can be derived from changes in absorption. A variety of tissue types are described here as well as the absorption properties of their constituents.

3.1 Water

The researchers found that the percentage of water in the breasts under magnetic resonance imaging (MRI) assessment indicates that there is a strong correlation between The researchers found that the percentage of water in the breasts under magnetic resonance imaging (MRI) assessment indicates that there is a strong correlation between the percentage of water in the breast and the mammographic density, which is found to be significantly lower in older women than in younger women.[26] There is a variation in the amount of water in a woman's breasts, from 11% to 74%. Aging is associated with a decrease in water percentage.[26] A considerable amount of NIR light is absorbed by water due to its abundance. The absorption spectrum of water in the wavelength range of 600 - 1050 nm is presented in Fig. 2. Light can significantly transmit through the tissue from the wavelength of 200 nm to about 935 nm. The absorption drops again beyond 1000 nm, however, there are currently no efficient light detectors available at such longer wavelengths. Despite the low absorption coefficient of water between 200 and 935 nm, due to its high concentration in biological tissue, it still contributes significantly to attenuation.

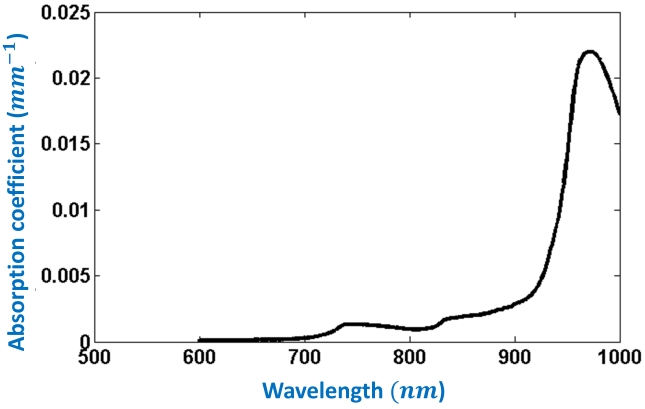

Figure 2. The absorption spectrum of pure water.

3.2 Lipids

Lipid or fat makes up about 80% of the women's breast weight.[17] Underneath the skin, the female breast comprises 50% glandular tissue and 50% adipose tissue by weight.[27] Cerussi et al.[28] reported the breast consisted of lipid fraction, 26% - 90%. Figure 3 represents the absorption spectrum of pork fat,[29] which is considered to be very similar to that of human lipids. At shorter wavelengths, the absorption coefficient is similar to that of water [Fig. 2], and a strong peak at a wavelength of about 930 nm. However, due to the low absorption of lipids in the NIR region, overall absorption is not significantly affected.

Preprints (www.preprints.org) | NOT PEER-REVIEWED | Posted: 12 December 2022 doi:10.20944/preprints202212.0187.v1

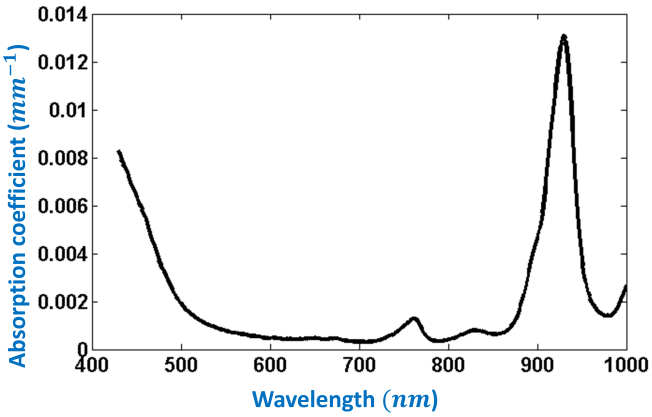

Figure 3. The absorption spectrum of pure fat.

3.3 Hemoglobin

Approximately 97% of the oxygen in the blood is carried by hemoglobin molecules in red blood cells (erythrocytes), while the remaining 3% is dissolved in plasma.[17,28,30] In the oxygenated state, hemoglobin is referred to as oxyhemoglobin (HbO_2), and in the reduced state, it is called de-oxyhemoglobin (Hb). Figure 4 shows the oxygen-hemoglobin dissociation curve,[31] which relates the percentage oxygen saturation of hemoglobin (SO2) to the partial pressure of oxygen dissolved in the blood (PO2).[28,30] The absorption coefficient spectra of pure oxy and deoxyhemoglobin are shown in Fig. 5. Absorption spectra of tissue with a composition similar to human postmenopausal breast[17] is shown in Fig. 6.

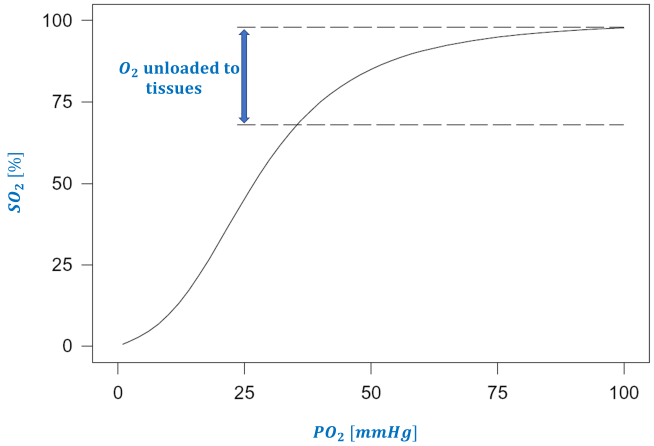

Figure 4. Oxygen-hemoglobin dissociation curve. Blood flowing out of the lungs has an oxygen saturation of about 97%, while venous blood is still about 67%. Hence during one cycle through the body, 30% hemoglobin-bound oxygen is released from the tissues.

Reconstructed optical properties are the spectroscopic variations in absorption and scattering coefficients.[32] A variety of metabolic or disease states of tissues can be diagnosed by reconstructing variations in optical properties, specifically, absorption coefficients.[33] This can be done by converting spectral variations in the absorption coefficient into useful functional data, such as total hemoglobin content and oxygen partial pressure. A malignant tumor's onset can be explained based on this information.[34]

Other tissue chromophores include melanin, cytochrome oxidase, myoglobin, and others. As they contribute little to the overall attenuation in the NIR region (but not in the visible region), they can be largely neglected. As shown in Fig. 6, breast tissue contains several different chromophores that absorb light;[17] the approximate

Preprints (www.preprints.org) | NOT PEER-REVIEWED | Posted: 12 December 2022 doi:10.20944/preprints202212.0187.v1

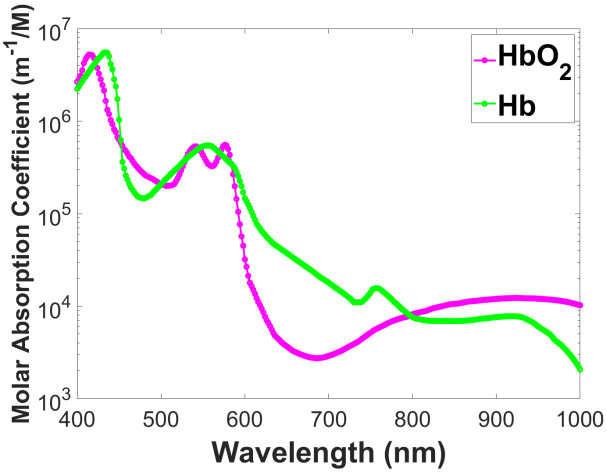

Figure 5. Absorption spectra of pure oxy and deoxyhemoglobin.

volume fraction, 15 μM oxyhemoglobin, 10 μM deoxyhemoglobin, water (15%), and fat (80%),[17] where μM is micro mole.

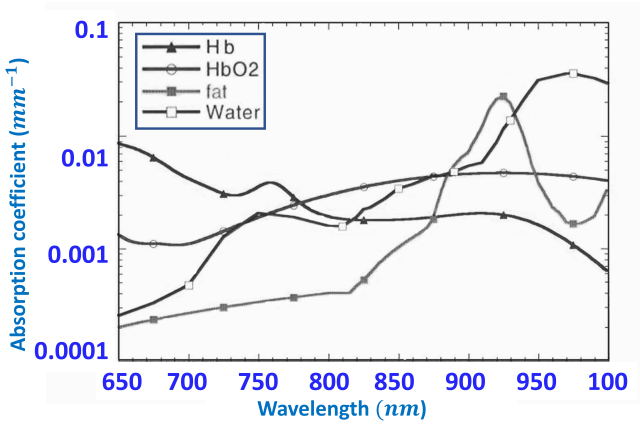

Figure 6. Absorption spectra of postmenopausal breast tissue with composition: 15 μM HbO_2, 10 μM Hb, fat (80% volume fraction), and water (15% volume fraction).

4. NIRS-BASED MEDICAL IMAGING

Diffuse optical tomography (DOT) is a medical imaging modality that uses the NIRS method to image internal structural maps and functional information of tissue.[35,36] The DOT system uses a model-based image reconstruction method to reconstruct the image and is also capable of measuring important chromophores as explained in Section 3, such as hemoglobin, water, and lipid inside the tissue. The Near-Infrared (NIR) method probes the optical properties of imaging tissues by transmitting or reflecting the NIR light from deep tissue. There are various multiplexing techniques that are used for high-speed switching of the light sources and detector,[37] as well as for data acquisition and calibration of hardware in order to correct errors that may have occurred during imaging.[38] Optical tomographic images can be reconstructed from measurement data. Inverse problems involve retrieving the spatial distribution of tissue optical properties from measured data at the tissue boundary. Due to the wavelength-dependent absorption of light by tissue constituents, DOT can provide functional images of tissues by incorporating multiple wavelengths of light sources in the non-ionizing NIR spectrum (600-1000

 doi:10.20944/preprints202212.0187.v1

nm).[4] The inverse problem is nonlinear, ill-posed, and sometimes underdetermined, and solving it requires a high computational power.[35] High-speed algorithms for 3D DOT image reconstruction have, however, been developed.[39] For faster image reconstruction, GPUs were used and multiple GPUs together were also used.[40] Real-time DOT imaging was demonstrated.[41] There was a method presented for scanning a specific area of tissue at high-speed.[42] Researchers are trying to reduce the cost of DOT instruments by using LEDs and photodetectors.[43] Additionally, DOT has been shown to be useful as a point-of-care imaging system.[44,45] In some cases, the systems are developed with an educational purpose in mind.[46] There is a tendency to add noise from the superficial layers of the tissues to the signal from the deep layers of the tissues while collecting data. There was a demonstration of a superficial noise reduction technique for DOT based on an empirical method.[47]

Functional near-infrared spectroscopy (fNIRS) is another simplified imaging method based on NIRS that makes use of channel-wise measurements rather than full image reconstruction. fNIRS is mostly used for brain imaging. Brain imaging with fNIRS includes measurement of brain functions, for example, cognitive workload.[48] It is possible to build an fNIRS system with limited hardware. There was also a demonstration of an fNIRS patch for brain imaging.[49,50] Optodes in the fNIRS systems are light sources and detectors, and the quality of the signal depends on their design.[51] Researchers are also studying portable fNIRS systems.[44,52] Various technologies were incorporated in the development of next-generation fNIRS systems, like internet-of-things architectures.[53,53,54] Additionally, fNIRS can be used for real-time classification of brain activity using machine learning.[55,56] There is still much research to be done in this field and the potential for fNIRS for brain imaging is still in its infancy. Research in this field is growing and has significant potential for the future.

REFERENCES

[1] Yamada, Y., "Light-tissue interaction and optical imaging in biomedicine," *Annual Review of Heat Transfer* **6** (1995).

[2] Hebden, J. C., Arridge, S. R., and Delpy, D. T., "Optical imaging in medicine: I. experimental techniques.," *Physics in medicine and biology* **42**, 825–840 (5 1997).

[3] Saikia, M. J. and Kanhirodan, R., "Development of handheld near-infrared spectroscopic medical imaging system," *Biophotonics Congress: Optics in the Life Sciences Congress 2019 (BODA,BRAIN,NTM,OMA,OMP)* , DS1A.6, Optical Society of America (2019).

[4] Gibson, A. P., Hebden, J. C., and Arridge, S. R., "Recent advances in diffuse optical imaging," *Physics in Medicine and Biology* **50**, R1 (2005).

[5] Saikia, M. J., "A spectroscopic diffuse optical tomography system for the continuous 3d functional imaging of tissue -a phantom study," *IEEE Transactions on Instrumentation and Measurement* , 1 (2021).

[6] Benaron, D. A., Cheong, W. F., and Stevenson, D. K., "Tissue optics.," *Science (New York, N.Y.)* **276**, 2002–2003 (6 1997).

[7] Arridge, S. R., Cope, M., and Delpy, D. T., "The theoretical basis for the determination of optical pathlengths in tissue: temporal and frequency analysis," *Physics in Medicine and Biology* **37**, 1531–1560 (7 1992).

[8] Arridge, S. R., "Photon-measurement density functions. part i: Analytical forms," *Appl. Opt.* **34**, 7395–7409 (11 1995).

[9] Arridge, S. R. and Schweiger, M., "Photon-measurement density functions. part 2: Finite-element-method calculations," *Appl. Opt.* **34**, 8026–8037 (12 1995).

[10] Hielscher, A. H., Klose, A. D., and Hanson, K. M., "Gradient-based iterative image reconstruction scheme for time-resolved optical tomography," *Medical Imaging, IEEE Transactions on* **18**, 262–271 (3 1999).

[11] Cutler, M., "Transillumination as an aid in the diagnosis of breast lesions," *Surgery, gynecology and obstetrics* **48**, 721–729 (1929).

[12] Tromberg, B. J., Pogue, B. W., Paulsen, K. D., Yodh, A. G., Boas, D. A., and Cerussi, A. E., "Assessing the future of diffuse optical imaging technologies for breast cancer management.," *Medical physics* **35**, 2443–2451 (6 2008).

[13] Saikia, M. J. and Kanhirodan, R., "Region-of-interest diffuse optical tomography system," *Review of Scientific Instruments* **87**, 013701 (1 2016).

[14] Cheong, W. F., Prahl, S. A., and Welch, A. J., "A review of the optical properties of biological tissues," *IEEE Journal of Quantum Electronics* **26**, 2166–2185 (1990).

[15] Woodard, H. Q. and White, D. R., "The composition of body tissues.," *The British journal of radiology* **59**, 1209–1218 (12 1986).

[16] Cooper, A. P., [*On the Anatomy of the Breast*], vol. 1, Longman (1840).

[17] Tromberg, B. J., Shah, N., Lanning, R., Cerussi, A., Espinoza, J., Pham, T., Svaasand, L., and Butler, J., "Non-invasive in vivo characterization of breast tumors using photon migration spectroscopy.," *Neoplasia (New York, N.Y.)* **2**, 26–40 (2000).

[18] Srinivasan, S., Pogue, B. W., Jiang, S., Dehghani, H., Kogel, C., Soho, S., Gibson, J. J., Tosteson, T. D., Poplack, S. P., and Paulsen, K. D., "Interpreting hemoglobin and water concentration, oxygen saturation, and scattering measured in vivo by near-infrared breast tomography," *Proceedings of the National Academy of Sciences* **100**, 12349–12354 (2003).

[19] Delpy, D. T. and Cope, M., "Quantification in tissue near-infrared spectroscopy.," (6 1997).

[20] Vaupel, P., Kallinowski, F., and Okunieff, P., "Blood flow, oxygen and nutrient supply, and metabolic microenvironment of human tumors: a review.," *Cancer research* **49**, 6449–6465 (12 1989).

[21] Ishimaru, A., [*Wave propagation and scattering in random media*], vol. 2, Academic press New York (1978).

[22] Bohren, C. F. and Huffman, D. R., [*Absorption and scattering of light by small particles*], John Wiley and Sons (2008).

[23] Ishimaru, A., "Diffusion of light in turbid material," *Appl. Opt.* **28**, 2210–2215 (6 1989).

[24] Bolin, F. P., Preuss, L. E., Taylor, R. C., and Ference, R. J., "Refractive index of some mammalian tissues using a fiber optic cladding method.," *Applied optics* **28**, 2297–2303 (6 1989).

[25] Marquez, G., Wang, L. V., Lin, S. P., Schwartz, J. A., and Thomsen, S. L., "Anisotropy in the absorption and scattering spectra of chicken breast tissue.," *Applied optics* **37**, 798–804 (2 1998).

[26] Boyd, N., Martin, L., Chavez, S., Gunasekara, A., Salleh, A., Melnichouk, O., Yaffe, M., Friedenreich, C., Minkin, S., and Bronskill, M., "Breast-tissue composition and other risk factors for breast cancer in young women: a cross-sectional study.," *The Lancet. Oncology* **10**, 569–580 (6 2009).

[27] Bryant, R. J., Underwood, A. C., Robinson, A., Stephenson, T. J., and Underwood, J. C. E., "Determination of breast tissue composition for improved accuracy in estimating radiation doses and risks in mammographic screening," *The Breast* **7**, 95–98 (1998).

[28] Cerussi, A. E., Berger, A. J., Bevilacqua, F., Shah, N., Jakubowski, D., Butler, J., Holcombe, R. F., and Tromberg, B. J., "Sources of absorption and scattering contrast for near-infrared optical mammography.," *Academic radiology* **8**, 211–218 (3 2001).

[29] Conway, J. M., Norris, K. H., and Bodwell, C. E., "A new approach for the estimation of body composition: infrared interactance.," *The American journal of clinical nutrition* **40**, 1123–1130 (12 1984).

[30] Liao, G. L. and Palmer, G., "The reduced minus oxidized difference spectra of cytochromes a and a3.," *Biochimica et biophysica acta* **1274**, 109–111 (6 1996).

[31] Bartrum, R. J. and Crow, H. C., "Transillumination lightscanning to diagnose breast cancer: a feasibility study," *American Journal of Roentgenology* **142**, 409–414 (1984). doi: 10.2214/ajr.142.2.409.

[32] Taroni, P., Torricelli, A., Spinelli, L., Pifferi, A., Arpaia, F., Danesini, G., and Cubeddu, R., "Time-resolved optical mammography between 637 and 985 nm: clinical study on the detection and identification of breast lesions.," *Physics in medicine and biology* **50**, 2469–2488 (6 2005).

[33] Spinelli, L., Torricelli, A., Pifferi, A., Taroni, P., Danesini, G. M., and Cubeddu, R., "Bulk optical properties and tissue components in the female breast from multiwavelength time-resolved optical mammography," *Journal of Biomedical Optics* **9**, 1137–1142 (2004).

[34] Durduran, T., Choe, R., Yu, G., Zhou, C., Tchou, J. C., Czerniecki, B. J., and Yodh, A. G., "Diffuse optical measurement of blood flow in breast tumors," *Opt. Lett.* **30**, 2915–2917 (11 2005).

[35] Arridge, S. R., "Optical tomography in medical imaging," *Inverse Problems* **15**, R41 (4 1999).

[36] Saikia, M. J., "Design and development of a functional diffuse optical tomography probe for real-time 3d imaging of tissue," *Optical Tomography and Spectroscopy of Tissue XIV* **11639**, 213–218, SPIE (2021).

[37] Poorna, R., Kanhirodan, R., and Saikia, M. J., "Square-waves for frequency multiplexing for fully parallel 3d diffuse optical tomography measurement," *Optical Tomography and Spectroscopy of Tissue XIV* **11639**, 219–226, SPIE (2021).

[38] Saikia, M. J., "An embedded system based digital onboard hardware calibration for low-cost functional diffuse optical tomography system," *Optics and Biophotonics in Low-Resource Settings VII* **11632**, 1–8, SPIE (2021).

[39] Saikia, M. J., Kanhirodan, R., and Vasu, R. M., "High-speed gpu-based fully three-dimensional diffuse optical tomographic system," *International Journal of Biomedical Imaging* **2014** (2014).

[40] Saikia, M. J. and Kanhirodan, R., "High performance single and multi-gpu acceleration for diffuse optical tomography," *Proceedings of 2014 International Conference on Contemporary Computing and Informatics, IC3I 2014* , 1320–1323, Institute of Electrical and Electronics Engineers Inc. (1 2014).

[41] Saikia, M. J., Rajan, K., and Vasu, R. M., "3-d gpu based real time diffuse optical tomographic system," *Souvenir of the 2014 IEEE International Advance Computing Conference, IACC 2014* , 1099–1103, IEEE Computer Society (2014).

[42] Saikia, M. J. and Kanhirodan, R., "Development of dot system for roi scanning," *International Conference on Fibre Optics and Photonics, 2014* , T3A.4, Optical Society of America (OSA) (12 2014).

[43] Saikia, M., Manjappa, R., and Kanhirodan, R., "A cost-effective led and photodetector based fast direct 3d diffuse optical imaging system," *Progress in Biomedical Optics and Imaging - Proceedings of SPIE* **10412** (2017).

[44] Saikia, M., Besio, W., and Mankodiya, K., "Wearlight: Toward a wearable, configurable functional nir spectroscopy system for noninvasive neuroimaging," *IEEE Transactions on Biomedical Circuits and Systems* **13** (2019).

[45] Saikia, M. J., Mankodiya, K., and Kanhirodan, R., "A point-of-care handheld region-of-interest (roi) 3d functional diffuse optical tomography (fdot) system," *Optical Tomography and Spectroscopy of Tissue XIII* **10874**, 90, SPIE (3 2019).

[46] Saikia, M. J. and Kanhirodan, R., "A tabletop diffuse optical tomographic (dot) experimental demonstration system," *Optics and Biophotonics in Low-Resource Settings V* **10869**, 11, SPIE (2 2019).

[47] Saikia, M. J., Manjappa, R., Mankodiya, K., and Kanhirodan, R., "Depth sensitivity improvement of region-of-interest diffuse optical tomography from superficial signal regression," *Optics InfoBase Conference Papers* **Part F99-C**, CM3E.5, OSA - The Optical Society (6 2018).

[48] Saikia, M. J., Besio, W. G., and Mankodiya, K., "The validation of a portable functional nirs system for assessing mental workload," *Sensors* **21**, 3810 (2021).

[49] Abtahi, M., Cay, G., Saikia, M. J., and Mankodiya, K., "Designing and testing a wearable, wireless fnirs patch," *Proceedings of the Annual International Conference of the IEEE Engineering in Medicine and Biology Society, EMBS* **2016-Octob**, 6298–6301, Institute of Electrical and Electronics Engineers Inc. (10 2016).

[50] Saikia, M. J. and Mankodiya, K., "A wireless fnirs patch with short-channel regression to improve detection of hemodynamic response of brain," *3rd International Conference on Electrical, Electronics, Communication, Computer Technologies and Optimization Techniques, ICEECCOT 2018* , 90–96, Institute of Electrical and Electronics Engineers Inc. (12 2018).

[51] Saikia, M. and Mankodiya, K., "3d-printed human-centered design of fnirs optode for the portable neuroimaging," *Progress in Biomedical Optics and Imaging - Proceedings of SPIE* **10870** (2019).

[52] DigitalCommons, U. and Saikia, M. J., "A wearable, configurable functional near-infrared a wearable, configurable functional near-infrared spectroscopy system for wireless neuroimaging spectroscopy system for wireless neuroimaging,"

[53] Saikia, M. J., Cay, G., Gyllinsky, J. V., and Mankodiya, K., "A configurable wireless optical brain monitor based on internet-of-things services," *3rd International Conference on Electrical, Electronics, Communication, Computer Technologies and Optimization Techniques, ICEECCOT 2018* , 42–48, Institute of Electrical and Electronics Engineers Inc. (12 2018).

[54] Saikia, M. J., "Internet of things-based functional near-infrared spectroscopy headband for mental workload assessment," *Optical Techniques in Neurosurgery, Neurophotonics, and Optogenetics* **11629**, 143–150, SPIE (2021).

 doi:10.20944/preprints202212.0187.v1

[55] Saikia, M. J., Kuanar, S., Borthakur, D., Vinti, M., and Tendhar, T., "A machine learning approach to classify working memory load from optical neuroimaging data," 69 (2021).

[56] Saikia, M. J. and Brunyé, T. T., "K-means clustering for unsupervised participant grouping from fnirs brain signal in working memory task," *Optical Techniques in Neurosurgery, Neurophotonics, and Optogenetics* **11629**, 159–164, SPIE (2021).